SCIENTIFIC REPORTS

OPEN

SUBJECT AREAS:
ELECTRONIC MATERIALS AND DEVICES
POLYMERS AND SOFT MATERIALS
POLYMER CHEMISTRY
PHYSICAL CHEMISTRY

Received
1 June 2012

Accepted
10 August 2012

Published
24 August 2012

Correspondence and requests for materials should be addressed to A.S. (saeki@chem.eng.osaka-u.ac.jp) or S.S. (seki@chem.eng.osaka-u.ac.jp)

Fullerene nanowires as a versatile platform for organic electronics

Yuta Maeyoshi[1], Akinori Saeki[1,2], Shotaro Suwa[1], Masaaki Omichi[1], Hiromi Marui[1], Atsushi Asano[1], Satoshi Tsukuda[3], Masaki Sugimoto[4], Akihiro Kishimura[5], Kazunori Kataoka[5,6,7] & Shu Seki[1]

[1]Department of Applied Chemistry, Graduate School of Engineering, Osaka University, 2-1 Yamadaoka, Suita, Osaka 565-0871, Japan, [2]PRESTO, Japan Science and Technology Agency (JST), 4-1-8 Honcho Kawaguchi, Saitama 332-0012, Japan, [3]Institute of Multidisciplinary Research for Advanced Materials, Tohoku University, 2-1-1, Katahira, Aoba-ku, Sendai 980-8577, Japan, [4]Takasaki Advanced Radiation Research Institute, Japan Atomic Energy Agency, 1233 Watanuki-machi, Takasaki, Gunma 370-1292, Japan, [5]Department of Materials Engineering, [6]Department of Bioengineering, Graduate School of Engineering, The University of Tokyo, 7-3-1 Hongo, Bunkyo-ku, Tokyo 113-8656, Japan, [7]Division of Clinical Biotechnology, Center for Disease Biology and Integrative Medicine, Graduate School of Medicine, The University of Tokyo, 7-3-1 Hongo, Bunkyo-ku, Tokyo 113-0033, Japan.

The development of organic semiconducting nanowires that act as charge carrier transport pathways in flexible and lightweight nanoelectronics is a major scientific challenge. We report on the fabrication of fullerene nanowires that is universally applicable to its derivatives (pristine C_{60}, methanofullerenes of C_{61} and C_{71}, and indene C_{60} bis-adduct), realized by the single particle nanofabrication technique (SPNT). Nanowires with radii of 8–11 nm were formed via a chain polymerization reaction induced by a high-energy ion beam. Fabrication of a poly(3-hexylthiophene) (P3HT): [6,6]-phenyl C_{61} butyric acid methyl ester ($PC_{61}BM$) bulk heterojunction organic photovoltaic cell including $PC_{61}BM$ nanowires with precisely-controlled length and density demonstrates how application of this methodology can improve the power conversion efficiency of these inverted cells. The proposed technique provides a versatile platform for the fabrication of continuous and uniform n-type fullerene nanowires towards a wide range of organic electronics applications.

Currently, efforts to construct one-dimensional nanostructures of conjugated polymers[1,2] and molecules are implemented using techniques such as templating[3], electrodeposition[4], and self-assembly[5,6]. Fullerenes, which have spherical shapes, electron accepting and transport capability, have occupied an important place in photochemistry[7] and organic electronics[8]. They are electron and energy acceptors with rigid spherical π-conjugation, which provides an attractive avenue to applications in cosmetics, fluid lubrication, lightweight hard plastics, and organic electronics[9–12]. Recently, the emerging field of organic semiconductors has cast a prominent spotlight on fullerene derivatives, because they possess deep-lying lowest unoccupied molecular orbitals (LUMO), and consequently, a negative (n)-type semiconducting nature[13–15]. Bulk heterojunction (BHJ) organic photovoltaic cells (OPV) are a notable application, which consist of positive (p)-type conjugated polymers and n-type fullerene derivatives that provide a promising framework, allowing the formation of a bi-continuous network with a large p/n interface, so that high power conversion efficiency (PCE) can be achieved[16,17]. Although the soluble fullerenes represent major advances in BHJ architecture, the thermal instability of BHJs, due partly to the diffusive motion of molecular fullerenes, must be addressed to realize the practical application of OPV[18]. Therefore, fullerene nanowires with a robust structure, which secure a large interface of p/n junctions and electron transport to the cathode, would contribute to the realization of stable BHJs.

The single particle nanofabrication technique (SPNT)[19–22] was specifically designed to construct organic nanowires by irradiating a polymer thin film with high-energy charged particles, where "one" ion particle can deposit kinetic energy along the nanospace trajectory sufficient for the production of high-density radicals, with gelation resulting via cross-linking reactions. The subsequent development process dissolves the unexposed area and isolates the nanowires from the film material. Figure 1a shows a schematic of the procedure for nanowire formation. It is noteworthy that SPNT has universal applicability to various polymers; not only conventional polymers such as poly(styrene)[20], but also conjugated polymers such as poly(silane), poly(thiophene), and poly(fluorene)[21,22]. The prerequisite for nanowire formation is a higher efficiency for cross-linking than main-chain scission.

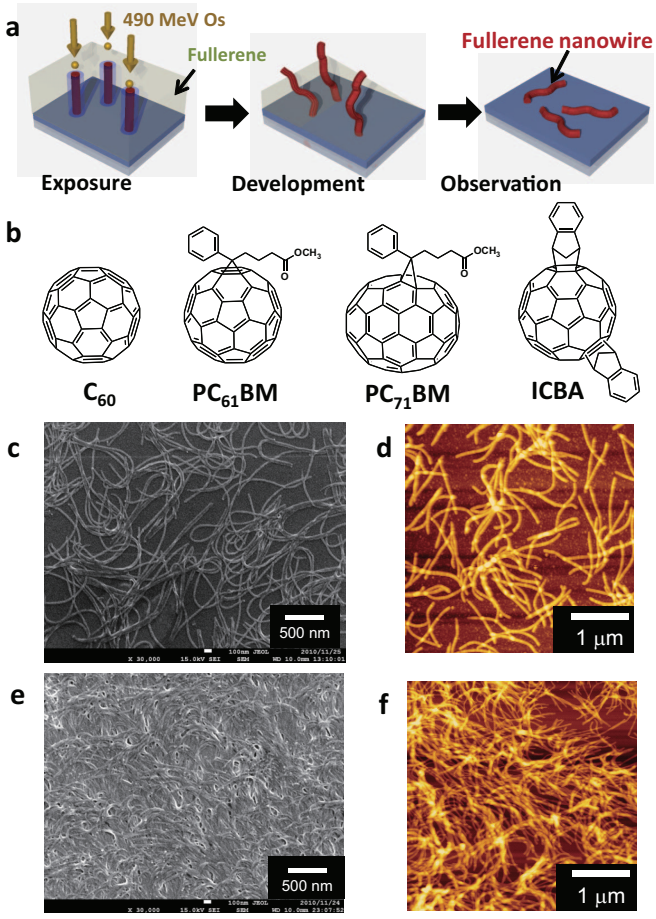

Figure 1 | Formation of fullerene derivative nanowires. (a) Schematic procedure for nanowire formation by SPNT; (left) irradiation of 490 MeV Os ions perpendicular to fullerene films, (center) development in CB or oDCB, where the non-irradiated area is dissolved, (right) nanowires formed are lying on the substrate. (b) Chemical structures of the fullerene derivatives used in the present study. (c) SEM and (d) AFM images of $PC_{61}BM$ nanowires (450 MeV Xe ions at 1.0×10^{9} ions cm^{-2} fluence). (e) SEM and (f) AFM images of $PC_{61}BM$ nanowires (450 MeV Xe ions at 1.0×10^{10} ions cm^{-2} fluence).

Although most p-type conjugated polymers have been successfully converted to nanowires by SPNT, the formation of conjugated molecule nanowires has remained elusive, because small molecules require a large number of cross-linking reactions to ensure insolubility against the developer. Thus, we have examined small n-type molecules, such as the fullerene derivatives shown in Fig. 1b.

Results

Nanowire formation of fullerene derivatives. SPNT was applied to films of C_{60}[23], [6,6]-phenyl C_{61} butyric acid methyl ester ($PC_{61}BM$)[16], [6,6]-phenyl C_{71} butyric acid methyl ester ($PC_{71}BM$), and indene-C_{60} bis-adduct (ICBA)[24,25], according to the procedure illustrated in Fig. 1a. The latter three fullerenes are typical, soluble fullerenes used in BHJs. $PC_{61}BM$ nanowires were successfully formed, as evidenced by the scanning electron microscopy (SEM) and atomic force microscopy (AFM) images shown in Fig. 1c and 1d. The density of the nanowires can be easily scaled up by simply increasing the ion beam fluence, as shown in Fig. 1e and 1f. The lengths of the nanowires are almost equivalent to the thickness of the original film (ca. 1 μm), and are independent of the ion fluence.

The respective dependence of the $PC_{61}BM$ nanowire length and density on the film thickness and ion fluence was examined. The lengths of the nanowires were always equivalent to the film thickness for various film thicknesses of 0.1, 0.5 and 4 μm (Supplementary Fig. S1). Furthermore, the number of nanowires observed in a 2×2 μm^2 AFM image area coincided with the number of incident ions calculated from the corresponding fluence (1.0, 3.0, and 5.0×10^{8} ions cm^{-2}) as shown in Supplementary Fig. S2. These results indicate that (1) nanowires are formed for each ion trajectory, (2) the terminus of a substrate-side nanowire is strongly connected to the bottom surface without separation during the development process, and (3) the fullerene nanowires do not swell in the longitudinal direction by contact with the development solvent.

The AFM images shown in Fig. 2a demonstrate that SPNT affords nanowires for all of the C_{60}, $PC_{61}BM$, $PC_{71}BM$, and ICBA fullerene derivatives. The histogram below each micrograph indicates the distribution of the nanowire radius, obtained using an ellipsoidal model and the measurement of one hundred points of height and width (see supplementary information). The averaged radii are summarized in Table 1. ICBA, which has a slightly larger radius (11 nm) than the other fullerenes (8–9 nm) and bears two bulky indene units, has been extensively utilized in BHJs in combination with regioregular poly(3-hexylthiophene) (P3HT), because the high LUMO of ICBA achieves a high open-circuit voltage (V_{oc}) for the OPV[24]. The bis-adduct fullerene has many regioisomers, which ensures good solubility, but may disrupt three-dimensional crystallization[25]. This could lead to increased radius and flexibility of the nanowires that reflects the packing in the fullerene film and its solubility. This presumption is strongly corroborated by the topography of the 2 μm-length nanowires made of bare C_{60}, whereas they are obviously rigid with a complete straight shape, in contrast to substituted fullerenes (Fig. 2b).

The scanning tunneling microscopy (STM) image of a C_{60} nanowire (Fig. 2c) reveals that the surface is covered by closely packed fullerene molecules. Dimerization and polymerization reactions of C_{60} have been reported with light exposure[26,27], high temperature and pressure[28], and γ-ray irradiation[29]. The 2+2 cycloaddition reaction (Fig. 2d) has been proposed for the photopolymerization reaction, as studied by Raman spectroscopy[27]. The STM images of the C_{60} nanowires on a Si substrate were also collected in a variety of bias voltage applied to the substrate (Supplementary Fig. S3). The optimized bias voltage was set at $-1\sim-1.2$ V for the clear visualization of the outer cage of C_{60} molecules (Fig. S3(d) ~ (f)), which was the considerably higher bias voltage required for the visualization of C_{60} molecules not polymerized into the nanowires and distributed on the surface (Fig. S3(a)~(c)). This is suggestive that the polymerization reaction at the surface of the nanowires causes lowering of the energy levels of LUMO orbital of C_{60} molecules bound into the nanowires. Taking account of these reports and the good mechanical strength of the nanowires, a similar polymerization reaction is also expected to occur for SPNT, in which nanowire formation is successful, regardless of the substituents.

Chain polymerization reaction. To produce a complete picture of the polymerization reaction, the cross-linking efficiency $G(x)$, was estimated and is defined by the number of reactions per 100 eV of absorbed ion dose. From the theoretical model, $G(x)$ is expressed as[20]:

$$G(x) = \frac{400\pi\rho N_A \cdot r^2}{LET \cdot M} \ln\left(\frac{e^{1/2} r_p}{r_c}\right), \qquad (1)$$

where ρ is the density of the material, N_A is Avogadro's number, r is the observed radius of the nanowire, LET is the linear energy transfer along the ion trajectory[30], M is the molecular weight, r_c and r_p are the respective radii of the core and penumbra areas given by the theoretical equation for collisions of charged particles with matter, and e is the elementary charge. This equation has been proven to be valid for many types of polymers[20–22]. $G(x)$ obtained for the fullerene nanowires are listed in Table 1 and range from 29 to 55 $(100\ eV)^{-1}$, which is approximately two orders of magnitude larger than that of

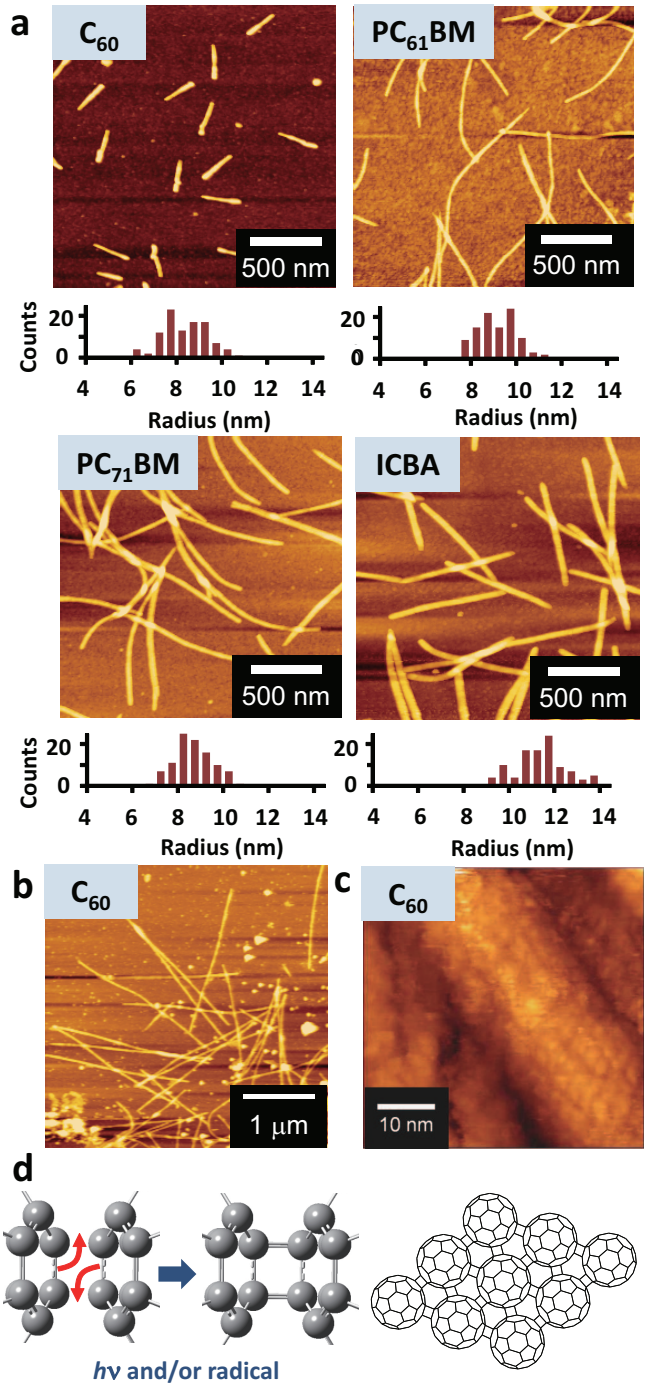

Figure 2 | Nanowire morphology. (a) AFM images of nanowires formed from fullerene derivatives by exposure to 490 MeV Os at 1.0×10^9 ions cm^{-2} fluence. The nanowire radius was estimated on the basis of an ellipsoidal model. See Table 1 for radii averaged from the histogram values. (b) AFM image of long and straight C_{60} nanowires. (c) STM image of C_{60} nanowires. (d) Proposed dimerization reaction via 2+2 cycloaddition[27]. The right schematic shows the expected structure of the polymerized fullerenes.

synthetic polymers such poly(4-bromostyrene), which has the highest $G(x)$ of 0.30–1.6 $(100\ eV)^{-1}$ among polymers[31]. Furthermore, $G(x)$ for the fullerene nanowires exceeds the initial ionization yield (ca. 5 $(100\ eV)^{-1}$)[32], which reveals that the polymerization reaction proceeds via a chain reaction.

p/n heterojunction of $PC_{61}BM$ and polyfluorene nanowires. Nanowire fabrication is facile in the direction perpendicular to the substrate; therefore, we attempted to form p/n junction nanowires comprising a p-type poly(9,9′-*n*-dioctylfluorene) (PFO) and n-type $PC_{61}BM$ bilayer. A bilayer without significant inter-mixing was successfully prepared by spin-coating a PFO layer from toluene solution onto a drop-cast $PC_{61}BM$ layer. Figure 3a shows a schematic of the procedure, where the bilayer is exposed to 450 MeV Xe ions and developed using toluene. The AFM image in Fig. 3b indicates nanowire formation, the length of which corresponds to the bilayer thickness. A magnified image of the nanowire (Fig. 3c) shows that the nanowire consists of two components; a straight, thick portion and a thin, winding portion. The size and morphology of the former portion are consistent with that observed for a $PC_{61}BM$ nanowire, and the latter portion appears identical to an individual PFO nanowire (Fig. 3d). There also appears to be an inflection point at the p/n heterojunction for several nanowires, which results from the difference in the mechanical strength of the PFO and $PC_{61}BM$ nanowires, as represented by the bottom right schematic in Fig. 3a. Furthermore, the rigidity of fullerene nanowires is evident from the low aspect ratio (width/height) of the $PC_{61}BM$ nanowire cross section, which is as small as 2.3, while that of PFO nanowires is 7.3. The PFO nanowires are flattened by either their own weight or by adhesive interaction with the surface. It should be noted that SPNT can be used to produce any type of semiconducting heterojunction with two dissimilar materials if a bilayer can be prepared. This toleration of SPNT towards materials is underlined by critical requisite for the formation of self-assembled nano-heterojunctions through synthetic procedure[33].

Table 1 | Nanowire radii *r*, and cross-linking efficiencies, *G(x)*

Fullerenes	*r* (nm)	*G*(*x*) ($(100\ eV)^{-1}$)
C_{60}	7.9±1.0	40
$PC_{61}BM$	8.6±0.8	36
$PC_{71}BM$	8.2±0.8	29
ICBA	10.9±1.1	55

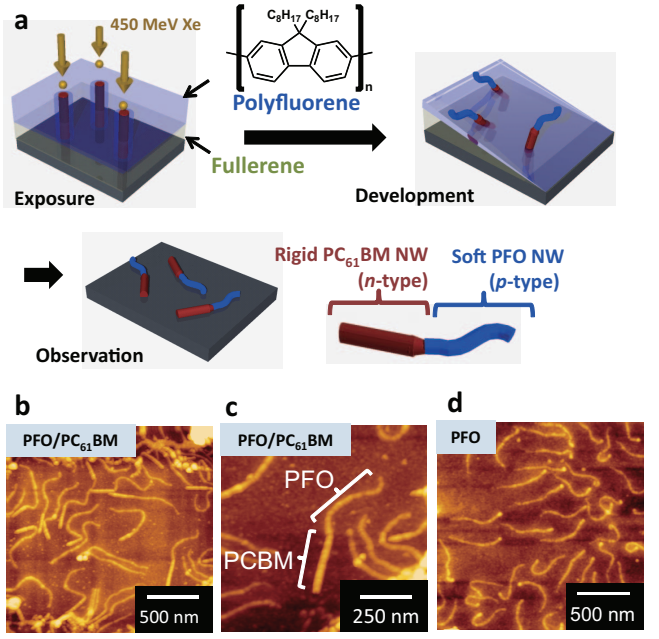

Figure 3 | Formation of pn-junction nanowires from a PFO/$PC_{61}BM$ bilayer. (a) Schematic showing the formation of pn-junction nanowires by SPNT from a PFO (upper) and $PC_{61}BM$ (lower) bilayer. (b, c) AFM images of PFO/$PC_{61}BM$ nanowires fabricated by exposure to 450 MeV Xe ions at a fluence of 1.0×10^9 ions cm^{-2}. (d) AFM image of PFO nanowires fabricated by exposure to 490 MeV Os ions at a fluence of 1.0×10^9 ions cm^{-2}.

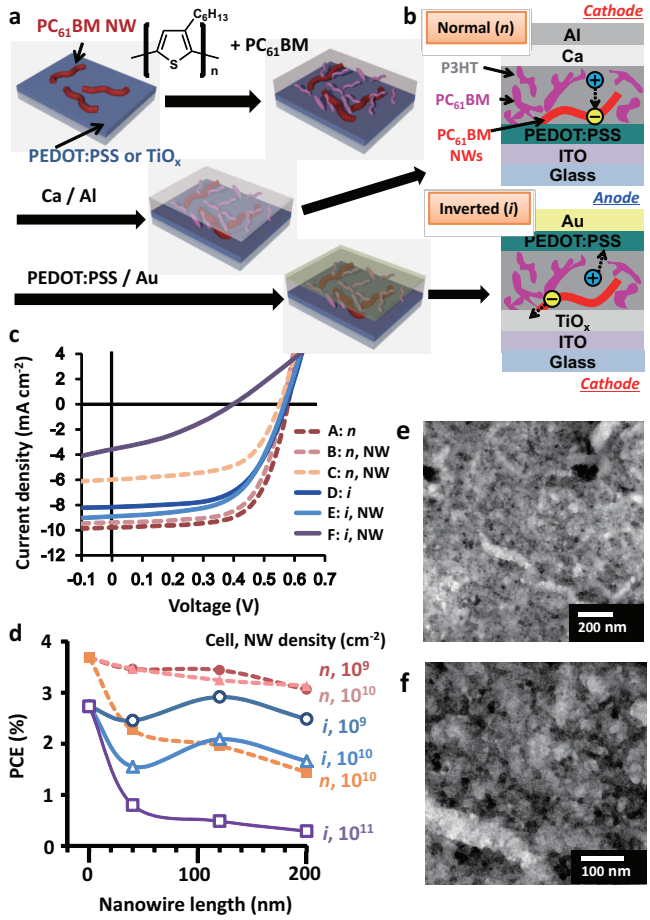

Figure 4 | Fabrication and characterization of the OPV device including $PC_{61}BM$ nanowires. (a) Schematic diagram of OPV fabrication. $PC_{61}BM$ nanowires (NWs) on the PEDOT:PSS or TiO_x layer were developed in CB and the P3HT:$PC_{61}BM$ BHJ layer was immediately spin-coated. Red and pink areas represent $PC_{61}BM$ NW and $PC_{61}BM$ domains, respectively, where the latter is formed from the addition of $PC_{61}BM$ molecules. (b) Schematic diagrams of normal (*n*) and inverted (*i*) OPVtructures. $PC_{61}BM$ NWs are concentrated on the lower layer. (c) *J-V* curves for the OPV devices. Dotted and solid lines represent the normal and inverted structures, respectively. $PC_{61}BM$ NWs (120 nm length) were formed by irradiation with 490 MeV Os ions. A: normal without $PC_{61}BM$ NWs, B: normal with $PC_{61}BM$ NWs (1.0×10^9 ions cm^{-2}), C: normal with $PC_{61}BM$ NWs (1.0×10^{11} ions cm^{-2}), D: inverted without $PC_{61}BM$ NWs, E: inverted with $PC_{61}BM$ NWs (1.0×10^9 ions cm^{-2}), and F: inverted with $PC_{61}BM$ NWs (1.0×10^{11} ions cm^{-2}). (d) PCE vs. NW length for each NW density (*n*: normal, *i*: inverted). (e, f) TEM images of the P3HT:PCBM film with $PC_{61}BM$ NW (1.0×10^{11} ions cm^{-2}).

Photovoltaic application of $PC_{61}BM$ nanowires. The p/n heterojunction demonstrated is expected to be applied for ideal charge separation and transport in OPV, or as a nanoscale diode for molecular switching, although integration of the p/n nanowires into the device still requires considerable development. Therefore, the hybridization of $PC_{61}BM$ nanowires with BHJ-type OPV was examined. Figures 4a and 4b show schematics for the fabrication of $PC_{61}BM$ nanowires on glass/ indium tin oxide (ITO)/ poly(3,4-ethylenedioxythiophene):poly(styrenesulfonate) (PEDOT:PSS) and glass/ITO/TiO_x substrates for normal and inverted cell structures[34]. The $PC_{61}BM$ nanowires were confirmed to be in contact with both substrate types. The active layer of P3HT:$PC_{61}BM$ = 1 : 1 w/w was spin-coated from *o*-dichlorobenzene (oDCB) solution in a nitrogen glove box, followed by solvent removal in a petri dish and thermal annealing at 150°C for 10 min. A PEDOT:PSS/Au anode and Ca/Al cathode layers were formed for the inverted and normal cells, respectively. The OPV performance was measured under illumination from an AM 1.5 G solar simulator. Figure 4c shows current density-voltage (*J-V*) curves for P3HT:$PC_{61}BM$ devices with and without $PC_{61}BM$ nanowires. The impact of nanowire length (L_{NW} = 40, 120, and 200 nm) and density (ρ_{NW} = 10^9, 10^{10}, and 10^{11} cm^{-2}) on the OPV performance was investigated. The PCE, V_{oc}, short-circuit current density (J_{sc}), and fill factor (FF) are listed in Table 2 (see Supplementary Fig. S4 for all *J-V* curves). When the nanowires are integrated with normal cells, the PCE was decreased from 3.68% without nanowires to 3.06% at ρ_{NW} = 10^9 cm^{-2} and to 1.44% at ρ_{NW} = 10^{11} cm^{-2}. The negative effect of the nanowires on the normal device is due to the connection of the n-type $PC_{61}BM$ nanowires to the anode ITO/PEDOT:PSS layer, so that electrons in the nanowires have a higher recombination rate with holes, which results in a significant drop of J_{sc} and FF. In contrast, the inverted cell with L_{NW} = 120 nm and ρ_{NW} = 10^9 cm^{-2} nanowires exhibited an approximate 7% improvement of the PCE over that without the nanowires (from 2.73 to 2.91%), due to an increase of J_{sc} (from 8.15 to 8.92 mA cm^{-2}) despite a slight decrease of the FF (59.3 to 57.7%). The segregation of $PC_{61}BM$ nanowires on the cathode ITO/TiO_x layer is beneficial for electron collection, which leads to an increase in the overall device performance (Fig. 4b).

Discussion

In the OPV devices, calculating the area that the nanowires with L_{NW} = 120 nm and ρ_{NW} = 10^9 cm^{-2} can cover gives a small value of only 2%. This may be an unprecedented finding that the nanowires act as seeds to promote the vertical segregation of $PC_{61}BM$ during the formation of active layer. The TEM images of BHJ with $PC_{61}BM$ nanowires reveals that the nanowire structures are preserved, although they seem larger than those before formation of the BHJ layer (Fig. 4e and 4f), which suggests the selective aggregation of $PC_{61}BM$ onto the seed nanowires. However, a high density of nanowires (ρ_{NW} > 10^{11} cm^{-2}) caused an abrupt decease in PCE, even for

Table 2 | Performance characteristics of P3HT:$PC_{61}BM$ = 1 : 1 OPV, with and without $PC_{61}BM$ nanowires

		NW density = 10^9 cm^{-2}				NW density = 10^{10} cm^{-2}				NW density = 10^{11} cm^{-2}			
Cell	NW length (nm)	PCE (%)	J_{sc} (mA cm^{-2})	V_{oc} (V)	FF (%)	PCE (%)	J_{sc} (mA cm^{-2})	V_{oc} (V)	FF (%)	PCE (%)	J_{sc} (mA cm^{-2})	V_{oc} (V)	FF (%)
Normal	0	3.68	9.69	0.575	66.2	3.68	9.69	0.575	66.2	3.68	9.69	0.575	66.2
Normal	40	3.46	9.60	0.562	64.1	3.47	9.25	0.567	66.2	2.27	7.31	0.554	56.1
Normal	120	3.44	9.38	0.564	65.1	3.25	8.94	0.563	64.5	1.96	5.98	0.550	59.5
Normal	200	3.06	8.63	0.553	64.1	3.14	8.68	0.550	65.6	1.44	4.66	0.556	55.7
Inverted	0	2.73	8.15	0.573	59.3	2.73	8.15	0.573	59.3	2.73	8.15	0.573	59.3
Inverted	40	2.45	8.34	0.547	53.7	1.55	7.78	0.489	40.8	0.80	4.92	0.445	36.6
Inverted	120	2.91	8.92	0.567	57.7	2.09	8.71	0.528	45.5	0.49	3.59	0.398	33.9
Inverted	200	2.48	8.27	0.557	53.9	1.66	7.67	0.509	42.5	0.29	1.85	0.447	34.9

the inverted cells (Fig. 4d), which suggests the nanowires have a negative effect.

The LUMO of $PC_{61}BM$ is considered slightly lowered in comparison with normal $PC_{61}BM$ along with narrowing of the band gap, on the basis of density functional theory results of C_{60} dimer[35,36]. In the characterization of photovoltaic devices (Table 2), V_{oc} is decreased with increasing the number density and length of $PC_{61}BM$ nanowires in the inverted cells, while it does not change significantly in the normal cells. This is the case giving that LUMO of $PC_{61}BM$ nanowires is also shifted downward as observed in C_{60} nanowires, because the electron energy level drops from the upper-lying LUMO of normal $PC_{61}BM$ domain to the lower-lying LUMO of $PC_{61}BM$ nanowires which are concentrated on the anode in the inverted cells.

It is difficult to yield bulk materials of $PC_{61}BM$ nanowires on the scale of a few milligrams for characterization of the electrical properties for devices such as field-effect transistors; therefore, electrodeless flash-photolysis time-resolved microwave conductivity (FP-TRMC)[37] was employed. The photoconductivity maxima of films exposed to fluences of 10^{10} and 10^{11} cm^{-2} were decreased by approximately 14 and 30%, respectively (Supplementary Fig. S5). Thus, the electron transport capability of the nanowires is worse than that of the pristine film due to the randomly-polymerized network, which is consistent with the results for the OPV, where too many nanowires resulted in degradation of the PCE. This result is, nonetheless, contradictory to that reported for a C_{60} film irradiated with 55–120 MeV ions and the formation of conductive pathways perpendicular to the substrate measured by conducting AFM[38]. However, the conditions used were different from the present study (conductive direction, method, ion beam energy, material, and development process), and thus more detailed investigations are highly anticipated. The negative effect on the OPV was found to manifest more in the normal P3HT:$PC_{61}BM$ cell with P3HT nanowires (L_{NW} = 200 nm, ρ_{NW} = 10^{11} cm^{-2}), of which the PCE was 0.53% with an extremely low FF of 27.1% (Supplementary Fig. S6), despite the preservation of the P3HT backbone and cross-linking of the side-chain, which are mainly responsible for the gelation.

The advantage of rigid fullerene nanowires over the bulk state is the thermal stability. The surface morphologies of $PC_{61}BM$ nanowires before and after thermal annealing at 160°C for 10 min were compared (Supplementary Figs. S7 and S8). The almost perfect conservation of the nanowire structure demonstrates the feasibility and stability of these organic electronics. State-of-the-art low bandgap copolymers comprising donor and acceptor units sometimes require fine-tuning of the side-chains and the incorporation of solvent additives such as 1,8-diiodeoctane to form an ideal BHJ network[39], whereas the present fullerene nanowires could pave the way towards the facile construction of BHJs with high thermal stability.

In spite of the relatively high mechanical strength of fullerene nanowires, they still lay down on the surface in the development process. Some uprisings are expected during the active layer coating; however, excessive long nanowires result in their bending and knocking down, which might be one of the reasons for the decrease of OPV performance observed in the long nanowires. Further investigations are on the way to making the nanowires stand on the surface by performing *dry* development process instead of the present *wet* process.

The simple concept of the present approach (a particle produces a corresponding nanowire) provides control of the number density of nanowires on a substrate, and the nanowires can be successfully applied as a versatile platform of continuous and uniform organic n-type semiconducting nanowires. The extremely high efficiency of the polycondensation reactions in fullerene derivatives may launch the single particle nanofabrication technique onto the industrial stage for application in the fabrication of electronic nanomaterials.

Methods

Formation of nanowires by SPNT. All reagents and chemicals were purchased from Nacalai Tesque, Inc. and Aldrich Chemical Co., Ltd. unless otherwise stated. The Si substrates were subjected to UV-ozone treatment. C_{60} was deposited on Si substrates by thermal evaporation in a vacuum chamber. $PC_{61}BM$, $PC_{71}BM$, and ICBA were dissolved in chlorobenzene (CB) and drop-cast on the Si substrate. Film thickness was measured using a stylus surface profiler (Ulvac, Dektak 150). Films were irradiated using 450 MeV Xe or 490 MeV Os particles from the cyclotron accelerator at the Takasaki Advanced Radiation Research Institute (TIARA) of the Japan Atomic Energy Agency. The number density of incident particles was controlled from 1.0×10^{8} to 1.0×10^{11} ions cm^{-2}. The irradiated C_{60} and fullerene derivative films were developed in oDCB and CB for 10 min, respectively. The loss of kinetic energy of particles due to penetration through the fullerene films was estimated using the SRIM 2010 calculation code[30].

Morphology observations. The size and shape of the nanowires were observed by atomic force microscopy (AFM; Seiko Instruments Inc., Nanocute OP and Nanonavi II) and scanning electron microscopy (SEM; Jeol Ltd., JSM-7001F). The surface structures of the C_{60} nanowires were measured using a scanning tunneling microscope (STM; Jeol Ltd., JSPM-5200). Transmission electron microscopy (TEM) observation was carried out using a Jeol Ltd. JEM-1400 microscope. The BHJ samples for TEM were prepared by exfoliation of a thin film layer after ultrasonication of a normal cell in water, which dissolves the bottom PEDOT:PSS layer and allows lift-off of the active layer with the nanowires.

OPV devices. *Materials:* Poly(3-hexylthiophene) (P3HT; >98% head-to-tail regioregularity, 99.995% trace metals basis, M_n = 3−6×10^4 g mol^{-1}, M_w/M_n < 2.5) and $PC_{61}BM$ (purity >99.5%) were purchased from Aldrich and Frontier Carbon, Inc., respectively. Solvents were purchased from Kishida Kagaku Corp. unless otherwise noted and were used as-received without further purification. PEDOT:PSS (Baytron P VP AI 4083) and ITO-coated glass substrates (<15 Ω $square^{-1}$) were purchased from H. C. Stark and Sanyo Shinku Corp., respectively. The ITO glass substrates were successively cleaned in tetrahydrofuran, detergent, de-ionized water, acetone, and isopropyl alcohol for 10 min each with ultrasonication. The dried ITO glass substrates were subjected to UV-ozone treatment.

Normal OPV: A PEDOT:PSS layer was cast onto the ITO layer by spin-coating after passing through a 0.2 μm filter. The substrate was annealed on a hot plate at 150°C for 30 min. A 2 wt% chloroform (CF) solution of $PC_{61}BM$ or 1.5 wt% CB solution of P3HT were cast on top of the PEDOT:PSS buffer layer in a nitrogen glove box by spin-coating or drop-casting after passing through a 0.2 μm filter. The films were then irradiated with 490 MeV Os particles. The number density of incident particles was controlled from 1.0×10^{9} to 1.0×10^{11} ions cm^{-2}. The irradiated films were developed in CB for 15 min in a nitrogen glove box. A 1.5 wt% oDCB solution of P3HT: $PC_{61}BM$ = 1 : 1 (w/w) was heated at 60°C with stirring for at least 4 h to achieve complete dissolution. The active layer was cast, immediately after development, on top of the PEDOT:PSS buffer layer in a nitrogen glove box by spin-coating at an optimized rotation speed and time after passing through a 0.2 μm filter. The films were annealed on a hot plate at 150°C for 10 min. A cathode consisting of 20 nm Ca and 100 nm Al layers was sequentially deposited through a shadow mask on top of the active layers by thermal evaporation in a vacuum chamber. The resulting device configuration was ITO (120–160 nm)/PEDOT:PSS (45–60 nm)/active layer (ca. 220 nm)/Ca (20 nm)/Al (100 nm) with an active area of 7.1 mm^2. Current-voltage (*J-V*) curves were measured using a source-measure unit (ADCMT Corp., 6241A) under AM 1.5 G solar illumination at 100 mW cm^{-2} (1 sun) using a 300 W solar simulator (SAN-EI Corp., XES-301S).

Inverted OPV: The TiO_x precursor (Koujundo Kagaku Corp.) was cast on the ITO layer by spin-coating after passing through a 0.2 μm filter. The layers were annealed on a hot plate at 150°C for 10 min. A 2 wt% CF solution of $PC_{61}BM$ was cast onto the TiO_x layer in a nitrogen glove box by spin-coating after passing through a 0.2 μm filter. The films were irradiated with 490 MeV Os particles, developed with CB, and the P3HT:$PC_{61}BM$ active layer was cast in a similar fashion to that for the normal OPV. An aqueous solution of PEDOT:PSS with 1 wt% poly(ethylene)glycol as a surfactant was dropped onto the active layer after passing through a 0.2 μm filter and immediately spin-coated. The layers were annealed on a hot plate at 150°C for 10 min. The anode consisted of a 50 nm Au layer that was deposited through a shadow mask on top of the active layers by thermal evaporation in a vacuum chamber. The resulting device configuration was ITO (120–160 nm)/TiO_x (ca. 10 nm)/active layer (ca. 220 nm)/PEDOT:PSS (50–100 nm)/Au (50 nm) with an active area of 7.1 mm^2. The *J-V* curves were measured in the same way as that for the normal OPV.

1. Zhao, Y. S., Wu, J. & Huang, J. Vertical Organic Nanowire Arrays: Controlled Synthesis and Chemical Sensors. *J. Am. Chem. Soc.* **131**, 3158–3159 (2009).
2. Ahn, J.-H., Kim, H.–S., Lee, K.J., Jeon, S., Kang, S.J., Sun, Y., Nuzzo, R, G. & Rogers, J. A. –Heterogeneous Three-Dimensional Electronics by Use of Printed Semiconductor Nanomaterials. *Science* **314**, 1754–1757 (2006).
3. O'Carroll1, D., Lieberwirth, I. & Redmond, G. Microcavity effects and optically pumped lasing in single conjugated polymer nanowires. *Nature Nanotech.* **2**, 180–184 (2007).
4. Ramanathan, K., Bangar, M. A., Yun, M., Chen, W., Mulchandani, A. & Myung, N. V. Individually Addressable Conducting Polymer Nanowires Array. *Nano Lett.* 4, 1237–1239 (2004).

5. Bullock, J. E., Carmieli, R., Mickley, S. M., Vura-Weis, J. & Wasielewski, M. R. Photoinitiated Charge Transport through π-Stacked Electron Conduits in Supramolecular Ordered Assemblies of Donor-Acceptor Triads. *J. Am. Chem. Soc.* **131**, 11919–11929 (2009).
6. Matsuo,Y., Sato, Y., Niinomi, T., Soga, I., Tanaka, H. & Nakamura, E. Columnar Structure in Bulk Heterojunction in Solution-Processable Three-Layered p-i-n Organic Photovoltaic Devices Using Tetrabenzoporphyrin Precursor and Silylmethyl[60]fullerene. *J. Am. Chem. Soc.* **131**, 16048–16050 (2009).
7. Imahori, H., Guldi, D. M., Tamaki, K., Yoshida, Y., Luo, C., Sakata, Y. & Fukuzumi, S. Charge Separation in a Novel Artificial Photosynthetic Reaction Center Lives 380 ms. *J. Am. Chem. Soc.* **123**, 6617–6628 (2001).
8. Chuvilin, A., Bichoutskaia, E., Gimenez-Lopez, M. C., Chamberlain, T. W., Rance, G. A., Kuganathan, N., Biskupek, J., Kaiser, U. & Khlobystov, A. N. Self-assembly of a sulphur-terminated graphene nanoribbon within a single-walled carbon nanotube. *Nature Mater.* **10**, 687–692 (2011).
9. Isaacson, C. W., Kleber, M. & Field, J. A. Quantitative Analysis of Fullerene Nanomaterials in Environmental Systems: A Critical Review. *Environ. Sci. Technol.* **43**, 6463–6474 (2009).
10. Sun, Y., Welch, G. C., Leong, W. L., Takacs, C. J., Bazan, G. C. & Heeger, A. J. Solution-processed small-molecule solar cells with 6.7% efficiency. *Nature Mater.* **11**, 44–48 (2012).
11. Chen, H.-Y., Hou, J., Zhang, S., Liang, Y., Yang, G., Yang, Y., Yu, L, Wu, Y & Li, G. Polymer solar cells with enhanced open-circuit voltage and efficiency. *Nature Photo.* **3**, 649–653 (2009)
12. Babu, S. S., Mohwald, H. & Nakanishi, T. Recent progress in morphology control of supramolecular fullerene assemblies and its applications. *Chem. Soc. Rev.* **39**, 4021–4035 (2010).
13. He, Z., Zhong, C., Huang, X., Wong, W.-Y., Wu, H., Chen, L., Su, S. & Cao, Y. Simultaneous Enhancement of Open-Circuit Voltage, Short-Circuit Current Density, and Fill Factor in Polymer Solar Cells. *Adv. Mater.* **23**, 4636–4643 (2011).
14. Beaujuge, P. M. & Fréchet, J. M. J. Molecular Design and Ordering Effects in π-Functional Materials for Transistor and Solar Cell Applications. *J. Am. Chem. Soc.* **133**, 20009–20029 (2011).
15. Clarke, T. M. & Durrant, J. R. Charge Photogeneration in Organic Solar Cells. *Chem. Rev.* **110**, 6736–6767 (2010).
16. Yu, G., Gao, J., Hummelen, J. C., Wudi, F. & Heeger, A. J. Polymer Photovoltaic Cells: Enhanced Efficiencies via a The device structure consisted of a Network of Internal Donor-Acceptor Heterojunctions. *Science* **270**, 1789–1791 (1995).
17. Service, R. F. Outlook Brightens for Plastic Solar Cells. *Science* **332**, 293-293 (2011).
18. Hishikawa, Y., Warta, W. & Dunlop, E. D. Solar cell efficiency tables (version 39). *Progress in Photovoltaics* **20**, 12–20 (2012).
19. Seki, S., Maeda, K., Tagawa, S., Kudoh, H., Sugimoto, M., Morita, Y. & Shibata, H. Formation of Nanowires along Ion Trajectories in Si Backbone Polymers. *Adv. Mater.* **13**, 1663–1665 (2001).
20. Seki, S., Tsukuda, S., Maeda, K., Matsui, Y., Saeki, A. & Tagawa, S. Inhomogeneous Distribution of Crosslinks in Ion Tracks in Polystylene and Polysilanes. *Phys. Rev. B* **70**, 144203/1–8 (2004).
21. Seki, S., Tsukuda, S., Maeda, K., Tagawa, S., Shibata, H., Sugimoto, M., Jimbo, K., Hashitomi, I. & Koyama, A. Effects of Backbone Configuration of Polysilanes on Nanoscale Structures Formed by Single-Particle Nanofabrication Technique. *Macromolecules* **38**, 10164 (2005).
22. Tsukuda, S., Seki, S., Sugimoto, M. & Tagawa, S. Customized Morphologies of Self-Condensed Multisegment Polymer Nanowires. *J. Phys. Chem. B* **110**, 19319–19322 (2006).
23. Kroto, H. W., Heath, J. R., O'Brien, S. C., Curl, R. F. & Smalley, R. E. C_{60}: Buckminsterfullerene. *Nature* **318**, 162–163 (1985).
24. Zhao, G., He, Y. & Li, Y. 6.5% Efficiency of Polymer Solar Cells Based on poly(3-hexylthiophene) and Indene-C_{60} Bisadduct by Device Optimization. *Adv. Mater.* **22**, 4355–4358 (2010).
25. Kang, H., Cho, C.-H., Cho, H.-H., Kang, T. E., Kim, H. J., Kim, K.-H., Yoon, S. C. & Kim, B. J. Controlling Number of Indene Solubilizing Groups in Multiadduct Fullerenes for Tuning Optoelectronic Properties and Open-Circuit Voltage in Organic Solar Cells. *ACS Appl. Mater. Interfaces* **4**, 110–116 (2012).
26. Rao, A. M., Zhou, P., Wang, K.-A., Hager, G. T., Holden, J. M., Wang, Y., Lee, W.-T., Bi, X.-X., Eklund, P. C., Cornett, D. S., Duncan, M. A. & Amster, J. Photoinduced Polymerization of Solid C_{60} Films. *Science* **259**, 955 (1993).
27. Zhou, P., Dong, Z. –H., Rao, A. M. & P. C. Eklund. Reaction mechanism for the photopolymerization of solid fullerene C_{60}. *Chem. Phys. Lett.* **211**, 337–340 (1993).
28. Iwasa, Y., Arima, T., Fleming, R. M., Siegrist, T., Zhou, O., Haddon, R. C., Rothberg, L. J., Lyons, K. B., Carter Jr, H. L. Hebard, A. F., Tycko, R., Dabbagh, G., Krajewski, J. J., Thomas, G. A. & Yagi, T. New Phases of C_{60} Synthesized at High Pressure. *Science* **264**, 1570–1572 (1994).
29. Malik, S., Fujita, N., Mukhopadhyay, P., Goto, Y., Kaneko, K., Ikeda, T. & Shinkai, S. Creation of 1D [60]fullerene superstructures and its polymerization by γ-ray Irradiation. *J. Mater. Chem.* **17**, 2454–2458 (2007).
30. The *G(x)* was obtained from each radius, molecular weight, density (1.5–1.7 g cm^{-3}), and linear energy transfer (*LET*) of 490 MeV Os (ca. 17–18 keV nm^{-1}) calculated by SRIM 2010 simulation code (http://www.srim.org/).
31. Burlant, W., Neerman, J. & Serment, V. γ-radiation of p-substituted polystyrenes. *J. Polym. Sci.* **58**, 491–500 (1962).
32. Hatano, Y., Katsumura, Y., & Mozumder, A. Charged Particle and Photon Interactions with Matter, -Recent Advances, Applications, and Interfaces; CRS Press (2011).
33. Zhang, W., Jin, W., Fukushima, T., Saeki, A., Seki, S. & Aida, T. Supramolecular Linear Heterojunction Composed of Graphite-Like Semiconducting Nanotubular Segments. *Science* **334**, 340–343 (2011).
34. Park, S. H., Roy, A., Beaupré, S., Cho, S., Coates, N., Moon, J. S., Moses, D., Leclerc, M., Lee, K. & Heeger, A. J. Bulk heterojunction solar cells with internal quantum efficiency approaching 100%. *Nature Photo.* **3**, 297–303 (2009).
35. Bihlmeier, A., Samson, C. C. M. & Klopper, W. DFT Study of Fullerene Dimers. *ChemPhysChem* **6**, 26252632– (2005).
36. Ren, T., Sun, B., Chen, Z., Qu, L., Yuan, H., Gao, X., Wang, S., He, R., Zhao, R., Zhao, Y., Liu, Z. & Jing, X. Photochemical and Photophysical Properties of Three Carbon-Bridged Fullerene Dimers: C_{121} (I, II, III). *J. Phys. Chem. B* **111**, 6344–6348 (2007).
37. Saeki, A., Tsuji, M. & Seki, S. Direct Evaluation of Intrinsic Optoelectronic Performance of Organic Photovoltaic Cells with Minimizing Impurity and Degradation Effects. *Adv. Energy Mater.* **1**, 661–669 (2011).
38. Kumar, A., Avasthi, D. K., Tripathi, A., Kabiraj, D., Singh, F. & Pivin, J. C. Synthesis of confined electrically conducting carbon nanowires by heavy ion irradiation of fullerene thin film. *J. Appl. Phys.* **101**, 014308/1–5 (2007).
39. Lee, J. K., Ma, W. L., Brabec, C. J., Yuen, J., Moon, J. S., Kim, J. Y., Lee, K., Bazan, G. C. & Heeger, A. J. Processing Additives for Improved Efficiency from Bulk Heterojunction Solar Cells. *J. Am. Chem. Soc.* **130**, 3619–3623 (2008).

Acknowledgments

This work was supported by the Japan Society for the Promotion of Science (JSPS) Funding Program for Next-Generation World-Leading Researches (NEXT Program), the Precursory Research for Embryonic Science and Technology (PRESTO) program of the Japan Science and Technology Agency (JST), and a KAKENHI grant from the Ministry of Education, Culture, Sports, Science and Technology (MEXT) of Japan. TEM measurements were conducted in the Research Hub for Advanced Nano Characterization, the University of Tokyo, supported by MEXT of Japan.

Author contributions

A.S. and S.Se. conceived and designed the research. Y.M. and S.Su. performed experiments, and H. M., A. A., M.O., S.T., and M.S. helped with experiments of ion beam irradiations. A.K. and K.K. conducted TEM experiments. Y.M., A.S., and S.Se. analysed the data and wrote the manuscript. All authors read and discussed it extensively.

Additional information

Supplementary information accompanies this paper at http://www.nature.com/scientificreports

Competing financial interests: The authors declare no competing financial interests.

How to cite this article: Maeyoshi, Y. *et al.* Fullerene nanowires as a versatile platform for organic electronics. *Sci. Rep.* **2**, 600; DOI:10.1038/srep00600 (2012).